Available online at www.sciencedirect.com
ScienceDirect
Journal of Bionic Engineering 5 (2008) 1−11

# Two-Dimensional Aerodynamic Models of Insect Flight for Robotic Flapping Wing Mechanisms of Maximum Efficiency

**Thien-Tong Nguyen[1], Doyoung Byun[2]**

1. *Department of Aeronautical Engineering*, *Hochiminh City University of Technology*, *Hochiminh City*, *Vietnam*
2. *Department of Aerospace Engineering*, *Konkuk University*, *Seoul* 143–701, *Korea*

**Abstract**

In the "modified quasi-steady" approach, two-dimensional (2D) aerodynamic models of flapping wing motions are analyzed with focus on different types of wing rotation and different positions of rotation axis to explain the force peak at the end of each half stroke. In this model, an additional velocity of the mid chord position due to rotation is superimposed on the translational relative velocity of air with respect to the wing. This modification produces augmented forces around the end of each stroke. For each case of the flapping wing motions with various combination of controlled translational and rotational velocities of the wing along inclined stroke planes with thin figure-of-eight trajectory, discussions focus on lift-drag evolution during one stroke cycle and efficiency of types of wing rotation. This "modified quasi-steady" approach provides a systematic analysis of various parameters and their effects on efficiency of flapping wing mechanism. Flapping mechanism with delayed rotation around quarter-chord axis is an efficient one and can be made simple by a passive rotation mechanism so that it can be useful for robotic application.

**Keywords**: bionics, modified quasi-steady approach, insect flight, hovering, forward flight



## 1 Introduction

Recent interest in the development of micro air vehicles with high aerodynamic performance has led aerodynamicists, biologists, robotic engineers to carry out numerous experimental and numerical research to explain the flapping mechanism of lift enhancement in insect flights[1,2]. Owing to the failure of early quasi-steady approaches in estimating sufficient forces required for hovering, the importance of unsteady effects that might explain the high forces produced by flapping wings has been recognized[3,4].

The wing stroke kinematics of an insect typically consists of four portions: two translational phases (down-stroke and up-stroke) when the wing sweeps through the air at high angle of attack, and two rotational phases (pronation and supination) when the wings rapidly rotate and reverse direction. The experimental results of Dickinson *et al*.[3] reveal that the rotational mechanisms are responsible for the high force peaks at the start and end of each half stroke.

In his review of the insect flight literature[5], Ellington based on a wide survey of data available at the time, convincingly argued that in most cases the existing quasi-steady theory fell short of calculating even the required average lift for hovering, and a substantial revision of the quasi-steady state theory is therefore necessary. Furthermore, Dickinson *et al*.[3,6,7] proposed that the existing quasi-steady state approach must be revised to include wing rotation in addition to flapping translation, as well as many unsteady mechanisms that might operate.

In the "modified quasi-steady" approach of this paper, 2D aerodynamic models of the flapping wing motions are analyzed with focus on types of rotation and the position of wing's rotation axis to explain the force peaks at the end of each half stroke. In this model, an additional velocity of the air relative to the mid chord position due to rotation is superimposed to the translational relative velocity of the air with respect to the wing.

**Corresponding author:** Thien-Tong Nguyen
**E-mail:** nguyentong@hcm.vnn.vn

This modification produces augmented forces around the end of each stroke. Instantaneous aerodynamic forces and power are computed based on lift and drag coefficients of thin airfoils at low Reynolds number[8,9]. Time-average values of non-dimensional forces and power are calculated for efficiency analysis.

The mechanisms of lift enhancement in insect flight have been investigated experimentally by visualization of air flows around flying insects recorded by high speed camera. Various kinds of insects such as beetles have been investigated and video images of flapping wing motion of these insects were analyzed to find their various flapping mechanisms. The most common and simple flapping wing motions are along inclined stroke planes with thin figure-of-eight trajectory and can be applied for robotic flapping wing mechanisms.

The wing kinematics for 2D model is described in details in the following section.

## 2 Description of wing kinematics

The wing flapping motion of insects could be considered as that of a propeller of radius $R_0$ rotating in the stroke plane but by an angular reciprocating motion of wing-beat amplitude $\phi$. The mean radius $R_m$ is about 70% of the wing length $R_0$ and the corresponding reciprocating distance traveled by the leading edge of the wing is the stroke amplitude $A_s$ as shown in Fig. 1.

The 2D insect wing is modeled by a symmetric airfoil of very small thickness. It follows a flapping motion along a thin figure-of-eight trajectory in the stroke plane of inclination $\beta$ with respect to the horizontal plane as illustrated in *oxy* plane in Fig. 2. The stroke amplitude $A_s$ varies from 2.5 to 5 times of the wing chord $c$. The wing section is represented by a straight line with filled circle at the leading edge. Other geometrical parameters include chord length $c$, stroke amplitude of translational phase $A_t$, stroke amplitude for rotational phase $0.5A_r$ at each end of the stroke, angle of chord inclination $\alpha_s$ with the stroke plane, angle of translational path inclination $\theta$ to the stroke plane of the figure-of-eight trajectory. The flapping kinematics considered in this paper are idealized. The translational velocity is denoted by $U_t$, which takes a constant value $U_{max}$ along FA and CD except near the beginning and

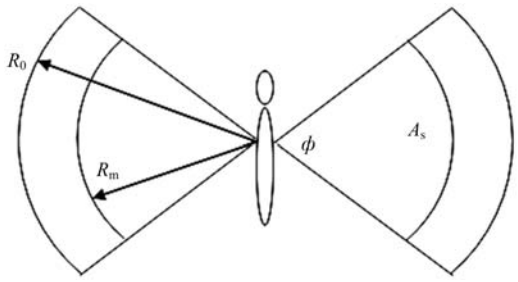


**Fig. 1** Flapping wing geometry.

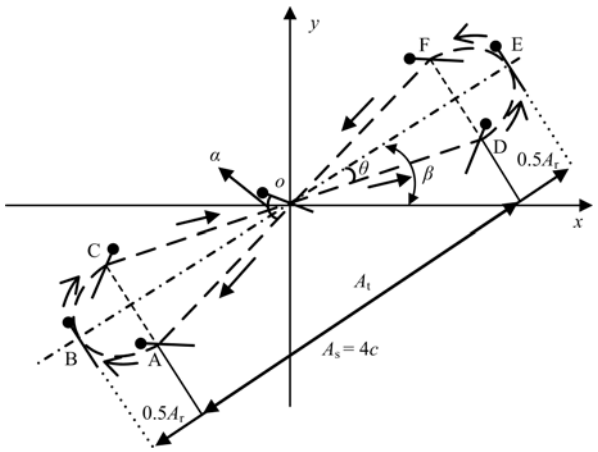


**Fig. 2** Flapping wing motion.

near the end of a stroke. During the rotational phases along ABC and DEF the wing follows a semi-elliptic path. The translational velocity component along the stroke plane $U_x$ decreases gradually to zero at the end of the stroke and reverses its value for the next stroke. The reference velocity is denoted by $U_{mean}$, which is the average stroke velocity of the whole flapping wing cycle.

The wing starts the down-stroke translational phase along FA with constant translational velocity $U_t$ and constant angle of inclination $\alpha_{s0}$ with the stroke plane. During the supination rotational phase along ABC, the translational velocity decreases along AB to zero at the end of down-stroke, then it increases again at the start of the up-stroke BC, while the angular velocity of the wing starts augmenting from zero at the end of translational phase A through B to C for adjusting the wing at the appropriate setting angle for the upstroke. The upstroke translational phase is followed along CD. Pronation rotational phase is then performed along DEF and a final translational down-stroke phase along FO to complete one wing stroke cycle.

From Fig. 2, different forms of wing trajectory can be obtained by changing the geometry parameters. A horizontal stroke plane is obtained when the stroke angle $\beta$ is equal to zero. The simplest trajectory along a straight line is when $\theta$ is equal to zero. A main variable of interest in this study is the time ratio between steady translational phase interval and total time of each stroke. The time ratio could vary from 0 to 1. Stroke plane inclined angle varies from 0˚ to 90˚ and wing inclination angle $\alpha_s$ varies from 0˚ to 90˚. Two different positions of rotation axis are considered, one is at mid chord and another is at 0.25$c$ from the leading edge of the wing. There are three types of rotation to be investigated:

(1) Symmetrical rotation: when the angle of chord inclination $\alpha_s$ with the stroke plane increases from a constant value $\alpha_{s1}$ of the translational phase to 90˚ at the end of the stroke amplitude and the wing chord continues to rotate until the angle of inclination equals another constant value $\alpha_{s2}$ at the start of the next translational phase.

(2) Advanced rotation: when angle of chord inclination $\alpha_s$ with the stroke plane makes the similar angle change for half of that rotating time to have the angle of inclination $\alpha_{s2}$ at the end of the stroke amplitude and the wing chord stops rotating until the next rotational phase near the other end of the stroke amplitude.

(3) Delayed rotation: when angle of chord inclination $\alpha_s$ remains the same constant value $\alpha_{s1}$ until the end of the stroke amplitude before making the similar angle change for half of that rotating time to have the angle of inclination $\alpha_{s2}$ at the start of the next translational phase.

## 3 Modified quasi-steady approach

For computation of quasi-steady lift and drag forces on the flapping wing, it is critical to have the correct velocity and angle of incidence of relative air with respect to the wing chord. In this "modified quasi-steady" approach, an additional velocity of the air due to rotation of the mid chord position is superimposed on the translational relative velocity of the air with respect to the chord. Induced velocities are calculated according to the theories of helicopter propeller and based on the wing's swept area, the insect's weight and its body's drag in horizontal forward flight. The component of total relative velocity due to rotation of the wing is calculated from the instantaneous angular velocity of the wing and the distance from the axis of rotation to the wing chord center. This velocity component due to wing rotation $V_{rotation}$ is normal to the wing chord, so that the instantaneous angular position of the wing chord must be known. Diagrams for velocities and forces are shown for various cases in Figs. 3–6. It is important to identify critical positions that cause changes in the direction of force components.

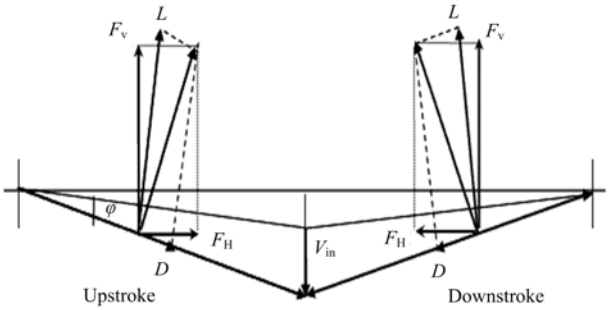


**Fig. 3** Velocities and forces in hovering flight with rotation axis at mid chord.

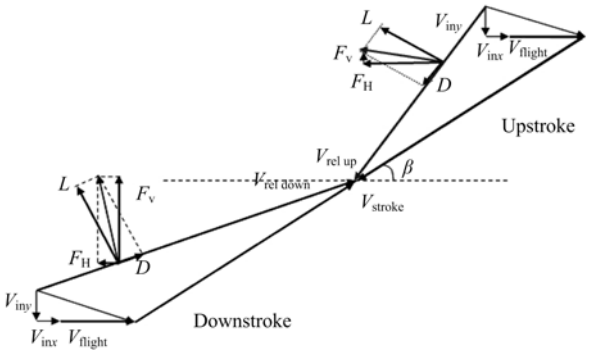


**Fig. 4** Velocities and forces in forward flight with rotation axis at mid chord.

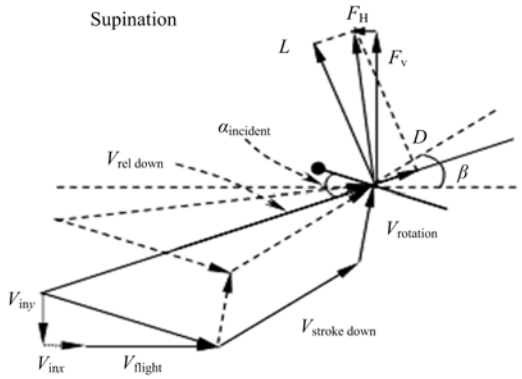


**Fig. 5** Velocities and forces on wing in supination with rotation axis near the leading edge.

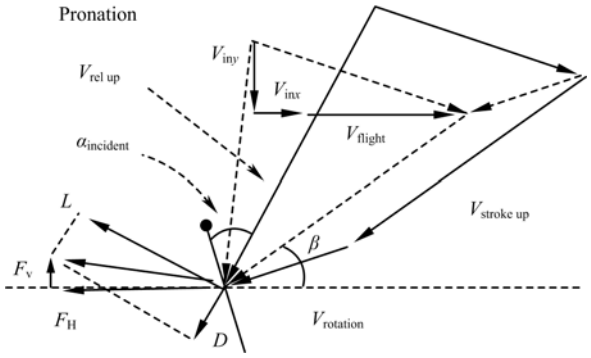


**Fig. 6** Velocities and forces on wing in pronation with rotation axis near the leading edge.

For a particular insect with known parameters such as weight $W$, mean wing chord $c$, wing length $R_0$, wing area $S_w$, wing-beat amplitude $\phi$, stroke amplitude $A_s$, swept area $S_s$ and wing beat frequency $f$, the vertical force coefficient based on average stroke velocity and wing area $S_w$ can be calculated. For 2D model, the wing flapping motion of insects could be considered as that at the mean radius $R_m$ of a propeller of radius $R_0$ rotating in the stroke plane. For a given time interval ratio between steady and unsteady translational wing motions of each stroke, the average stroke velocity $U_{mean}$ of the whole flapping wing cycle can be found. The ratio of forward velocity $V_{flight}$ to the average stroke velocity $U_{mean}$ is equivalent to the advance ratio $J$ in propeller theory.

From existing data available[1,4,10] and current experimental data, the vertical lift coefficient $C_v$ based on reference velocity $U_{mean}$ and wing area $S_w$ can be found to be from 0.74 to 1.40. In this paper, $C_v$ of 1.0 is chosen throughout quasi-steady computations.

For each case of flapping wing motions with various combinations of controlled translational and rotational velocities of the wing along inclined stroke planes with thin figure-of-eight trajectory, the vertical lift coefficient and horizontal force coefficient at numerous instants during one stroke cycle are computed. At each instant, the wing chord angular position and its angular velocity are defined corresponding to the selected type of rotation. For a chosen rotation axis of the wing, the velocity component due to rotation $V_{rotation}$ normal to the wing chord is then defined. The magnitude and direction of the resultant relative velocity of the air are computed from the velocity due to wing stroke motion along the inclined stroke planes with thin figure-of-eight trajectory, the forward flight velocity and vertical and horizontal induced velocities.

Instantaneous aerodynamic forces are calculated based on the incidence found and lift and drag coefficients of thin airfoils at low Reynolds number[8,9]. The best approximation of power of the wing can be found from the aerodynamic force along the stroke plane and the relative air velocity along this plane including a velocity component due to wing chord rotation, but assuming that frictional rotating power itself contributes only a small fraction. Time-average values of non-dimensional forces and power are calculated for efficiency analysis.

There are various lift and drag curves for thin airfoil at Reynolds number in the range of 200 – 5000[8–10]. Lift and drag coefficients for a wide range of angles of attack from 0° to 90° obtained by current unsteady computations for Reynolds number of 4000 are very similar to that of Dickinson and Gotz[9] for a Reynolds number of 2000. The results presented in Fig. 7 are used in this quasi-steady computation to take into account the unsteady effect of early translational stages of the wing.

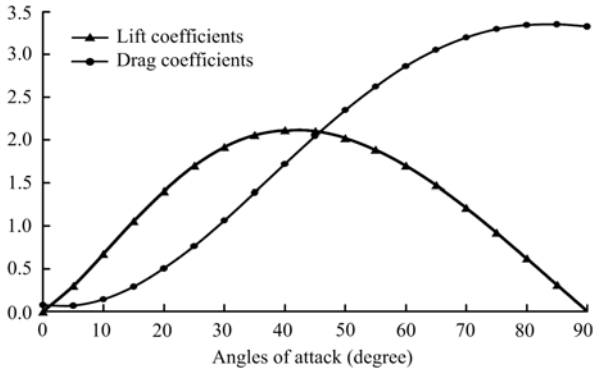


**Fig. 7** Lift and drag coefficients of thin aerofoil at Reynolds number of 4000.

## 4 Quasi-steady results for hovering flight

The computations of aerodynamic forces along a horizontal stroke plane of a 2D wing in hovering flight are carried out with stroke amplitude of 4$c$ and the base case of time ratio of 2/3 between steady translational phase interval and total time of each stroke. In this case the angle of inclination $\beta$ of the stroke plane is zero and advance ratio $J$ is also zero.

The average stroke velocity $U_{mean}$ is determined from parameters of flapping frequency $f$ and stroke amplitude $A_s$ at the mean radius $R_m$. The Reynolds number depends on this velocity and the wing chord. These parameters can be found from available data for insects[1,4,10]. The case of average Reynolds number about 4000 is chosen from the combination of these parameters. The vertical lift coefficient $C_v$ based on reference velocity $U_{mean}$ and wing area $S_w$ is chosen as 1.0 throughout quasi-steady computations. In hovering the corresponding horizontal force produced by the flapping wing cancels out in each complete stroke cycle.

The maximum translational velocity and the maximum angular velocity of the wing are then determined by the type of rotation and the time interval ratio between steady and unsteady translational wing motions of each stroke. An appropriate cosine function of translational velocity is assumed to give the required average stroke velocity $U_{mean}$ of the whole flapping wing cycle and the maximum value $U_{max}$ at the end and the beginning of each translational phase (Points A, C, D, F in Fig. 2) at the same time to give zero velocity at the end and beginning of each stroke (points B and E in Fig. 2). Velocity components of the wing along and normal to the stroke plane are shown in Fig. 8.

The instantaneous rotational velocity is then determined by additional information of the setting angles of chord inclination $\alpha_{s1}$ and $\alpha_{s2}$ with the stroke plane during translational phases. These setting angles of chord inclination $\alpha_{s1}$ and $\alpha_{s2}$ are variables used to find appropriate vertical lift coefficient, horizontal thrust coefficient and power coefficient produced by the flapping wing under pre-determined parameters.

The symmetrical, advanced and delayed rotations for two positions of the wing's rotation axis are investigated for the effect of rotation on peak forces at the end of each stroke. When the axis of wing rotation is at mid-chord position, the velocity component due to rotation $V_{rotation}$ normal to the wing chord is zero.

When the axis of wing rotation is at the quarter-chord position, the effect of rotation is indicated by peak vertical and horizontal forces near the end of each stroke, shown in Figs. 9 and 10. In the cases of advanced and delayed rotation the peak forces are much larger.

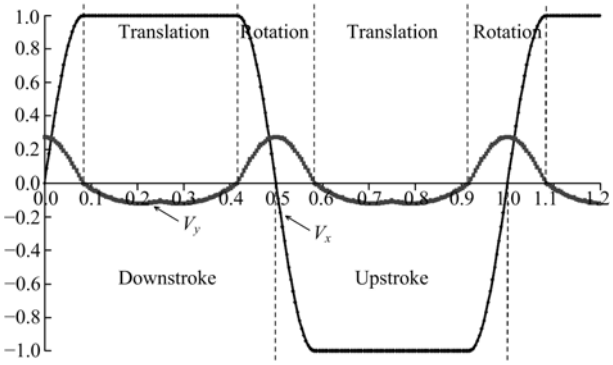


**Fig. 8** Velocity components of the wing along and normal to the stroke plane.

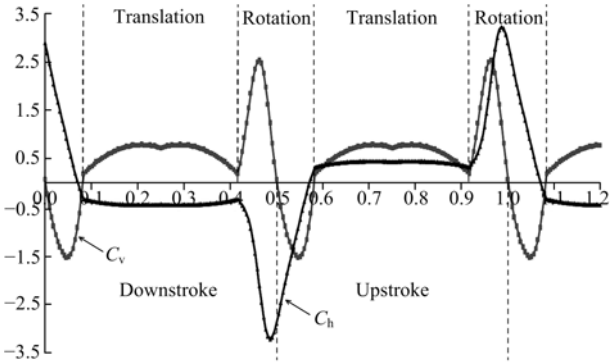


**Fig. 9** Vertical and horizontal force coefficients in hovering flight with symmetrical rotation.

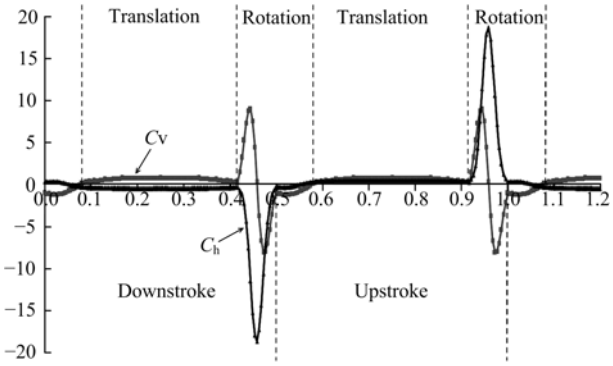


**Fig. 10** Vertical and horizontal force coefficients in hovering flight with advanced rotation.

While hovering with advanced rotation, at the end of translational phase the wing chord rapidly rotates to obtain the setting angle for the next stroke. Because of rotational effect, the vertical forces will first result in a positive force peak followed by a negative one due to an effective angle of attack of over 90° as the trailing edge faces the coming air. In the case of horizontal stroke plane for hovering flight the negative and positive

horizontal force coefficients for each half stroke cancel the opposite ones on the other half stroke.

Force coefficients of a wing in hovering flight with different types of rotation are plotted for comparison in Fig. 11 and Fig. 12. Very large peak forces are encountered in advanced rotation and hence very large power is required.

In Table 1, $\alpha_{s0}$ is the appropriate setting angle with respect to stroke plane in order to obtain the vertical force coefficient of 1.0. The results in Table 1 show that to sustain the same weight in hovering flight and with the axis of wing rotation at quarter-chord position, delayed rotation consumes about 86% of the power required by symmetrical rotation, while advanced rotation consumes 3.86 times more power. So it can be concluded that delayed rotation is the most efficient flapping mechanism in hovering flight with rotation axis at quarter-chord position.

To sustain the same weight in hovering flight with the axis of wing rotation at mid-chord position, the setting angles are slightly larger for all three types of wing rotation. However the results in Table 2 show that symmetrical rotation is the most efficient flapping mechanism in hovering flight with the rotational axis at the mid-chord position and it consumes only 80% of the power required by delayed rotation with the rotational axis at the quarter-chord position.

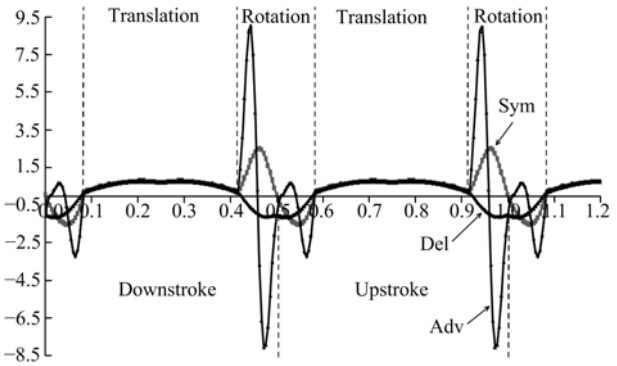


**Fig. 11** Vertical force coefficients in hovering flight with different types of rotation.

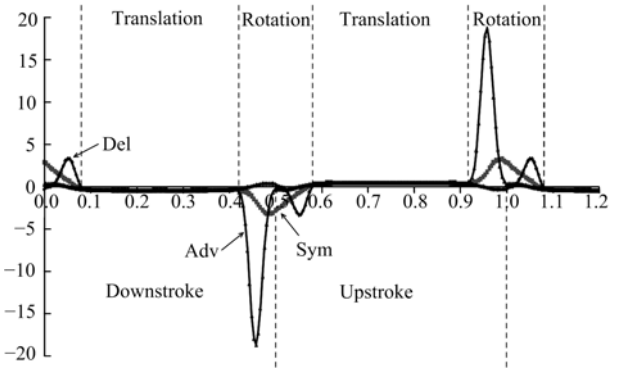


**Fig. 12** Horizontal force coefficients in hovering flight with different types of rotation.

**Table 1** Effect of types of rotation in hovering flight with rotation axis at quarter-chord position

| $\alpha_{s0}$ | $J=0$ | $C_v$ | $C_h$ | $C_p$ |
|---|---|---|---|---|
| | Symmetrical rotation | | $\beta=0^\circ$ | |
| 21°28 | Translation down | 1.22 | −0.49 | 0.56 |
| | Supination | 0.55 | −1.44 | 1.06 |
| 21°28 | Translation up | 1.22 | 0.49 | 0.56 |
| | Pronation | 0.55 | 1.44 | 1.06 |
| | Full-cycle average | 1.00 | 0.00 | 0.72 |
| | Advanced rotation | | $\beta=0^\circ$ | |
| 24°30 | Translation down | 1.50 | −0.68 | 0.77 |
| | Supination | 0.01 | −3.81 | 6.80 |
| 24°30 | Translation up | 1.50 | 0.68 | 0.77 |
| | Pronation | 0.01 | 3.81 | 6.80 |
| | Full-cycle average | 1.00 | 0.00 | 2.78 |
| | Delayed rotation | | $\beta=0^\circ$ | |
| 25°78 | Translation down | 1.62 | −0.78 | 0.88 |
| | Supination | −0.24 | −0.35 | 0.08 |
| 25°78 | Translation up | 1.62 | 0.78 | 0.88 |
| | Pronation | −0.24 | 0.35 | 0.08 |
| | Full-cycle average | 1.00 | 0.00 | 0.62 |

**Table 2** Effect of types of rotation in hovering flight with rotation axis at mid-chord position

| $\alpha_{s0}$ | $J=0$ | $C_v$ | $C_h$ | $C_p$ |
|---|---|---|---|---|
| | Symmetrical rotation | | $\beta=0^\circ$ | |
| 22°04 | Translation down | 1.30 | −0.53 | 0.61 |
| | Supination | 0.41 | 0.00 | 0.28 |
| 22°04 | Translation up | 1.30 | 0.53 | 0.61 |
| | Pronation | 0.41 | 0.00 | 0.28 |
| | Full-cycle average | 1.00 | 0.00 | 0.50 |
| | Advanced rotation | | $\beta=0^\circ$ | |
| 24°55 | Translation down | 1.52 | −0.69 | 0.79 |
| | Supination | −0.04 | 0.79 | 0.62 |
| 24°55 | Translation up | 1.52 | 0.69 | 0.79 |
| | Pronation | −0.04 | −0.79 | 0.62 |
| | Full-cycle average | 1.00 | 0.00 | 0.73 |
| | Delayed rotation | | $\beta=0^\circ$ | |
| 24°55 | Translation down | 1.52 | −0.69 | 0.79 |
| | Supination | −0.04 | 0.79 | 0.62 |
| 24°55 | Translation up | 1.52 | 0.69 | 0.79 |
| | Pronation | −0.04 | −0.79 | 0.62 |
| | Full-cycle average | 1.00 | 0.00 | 0.73 |

## 5 Quasi-steady results for forward flight

In forward flight, the horizontal force produced by a flapping wing overcomes the body drag of the insect. The body drag of a honey bee is around 10% of its weight for flight velocity from 3 $m \cdot s^{-1}$ to 4 $m \cdot s^{-1}$ [11,12]. This forward velocity is about 50% of the average stroke velocity $U_{mean}$ so that it is reasonable to assume that, in general, the body drag of insect is about 10% of its weight when the advance ratio $J = 0.5$. In the low Reynolds number region of insect flight, the body drag coefficient decreases slightly as flight velocity increases. The ratio of body drag of insect to its weight is equal to the ratio of the horizontal force coefficient to the vertical force coefficient. This force ratio varies with the advance ratio $J$ as shown in Fig. 13.

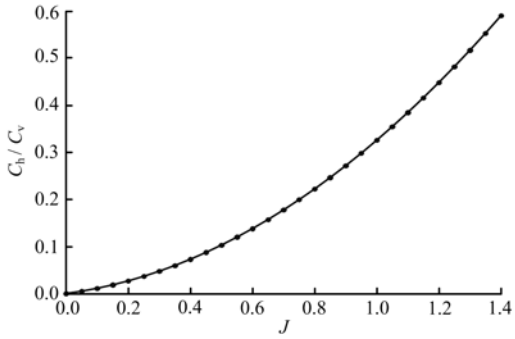


**Fig. 13** Variation of horizontal force coefficient with advance ratio $J$.

Quasi-steady computations for a two dimensional flapping wing in forward flight along an inclined stroke plane of various values of angle $\beta$ from 0° to 90° for symmetrical, advanced and delayed rotations around quarter-chord axis and mid-chord axis, with various values of advance ratio, are carried out with stroke amplitude of 4$c$ and time ratio of 2/3.

To sustain the same weight in forward flight at a given advance ratio $J$ and to produce the same corresponding horizontal force, inclined angles $\beta$ of stroke plane, setting angles $\alpha_{s1}$ and $\alpha_{s2}$ for the downstroke and upstroke of 2D flapping wing motion can be found for a specific type of wing rotation around a defined axis.

Vertical and horizontal force coefficients of a wing in forward flight with different types of rotation are plotted for comparison in Fig. 14 and Fig. 15. Advanced rotation produces very high vertical forces but also negative thrust in the supination phase. It also produces even larger negative vertical force and no thrust in the pronation phase as shown in Fig. 15.

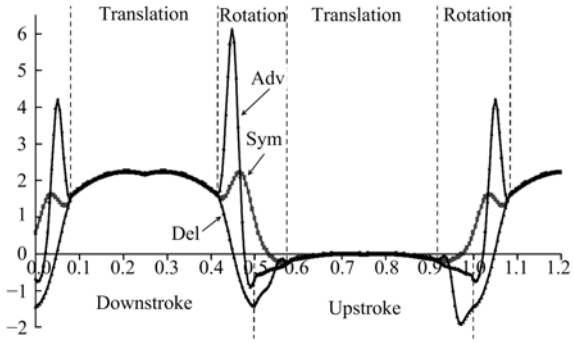


**Fig. 14** Vertical force coefficients on wing in forward flight with different types of rotation.

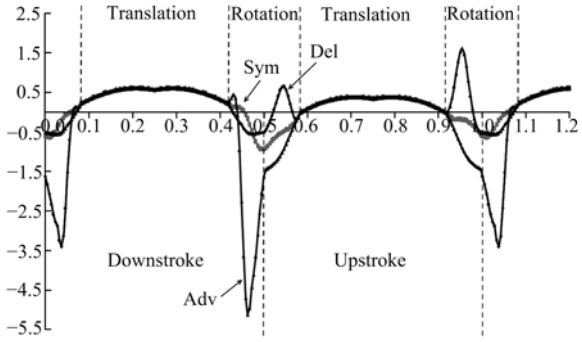


**Fig. 15** Horizontal force coefficients on wing in forward flight with different types of rotation

For an advance ratio $J = 0.5$ and inclined stroke angle $\beta = 45°$ solutions of different setting angles $\alpha_{s1}$ and $\alpha_{s2}$ are found for symmetrical, advanced and delayed rotations around the quarter-chord axis to produce the same vertical force $C_v = 1.0$ and the same corresponding horizontal force $C_h = 0.10$. The results are shown in Table 3.

To produce the same vertical force $C_v = 1.0$ and the same corresponding horizontal force $C_h = 0.10$ in forward flight with advance ratio $J = 0.5$, different inclined stroke angle $\beta$ and corresponding symmetrical setting angles $\alpha_{s1} = \alpha_{s2}$ are found for three types of rotation around the quarter-chord axis. The results are shown in Table 4.

In both cases, delayed rotation consumes 90% of power required by corresponding symmetrical rotation; however delayed rotation with symmetrical setting angles requires smaller inclined angle and slightly less power.

**Table 3** Effect of types of rotation around quarter-chord axis in forward flight with different setting angles

| $\alpha_{s0}$ | $J = 0.5$ | $C_v$ | $C_h$ | $C_p$ |
|---|---|---|---|---|
| | Symmetrical rotation | | $\beta = 45^\circ$ | |
| 28°47 | Translation down | 2.09 | 0.60 | 1.47 |
| | Supination | 2.15 | −1.50 | 2.21 |
| 23°45 | Translation up | −0.01 | 0.11 | 0.07 |
| | Pronation | −0.31 | 0.65 | 0.39 |
| | Full-cycle average | 1.00 | 0.10 | 0.95 |
| | Advanced rotation | | $\beta = 45^\circ$ | |
| 30°27 | Translation down | 2.40 | 0.63 | 1.75 |
| | Supination | 3.29 | −3.80 | 9.13 |
| 31°56 | Translation up | 0.12 | 0.60 | 0.28 |
| | Pronation | −2.33 | 1.91 | 4.23 |
| | Full-cycle average | 1.00 | 0.10 | 2.91 |
| | Delayed rotation | | $\beta = 45^\circ$ | |
| 33°25 | Translation down | 2.90 | 0.62 | 2.25 |
| | Supination | 0.33 | −0.77 | 0.36 |
| 27°66 | Translation up | 0.07 | 0.34 | 0.17 |
| | Pronation | −0.28 | −0.59 | −0.04 |
| | Full-cycle average | 1.00 | 0.10 | 0.86 |

**Table 4** Effect of types of rotation around quarter-chord axis in forward flight with symmetrical setting angles

| $\alpha_{s0}$ | $J = 0.5$ | $C_v$ | $C_h$ | $C_p$ |
|---|---|---|---|---|
| | Symmetrical rotation | | $\beta = 40^\circ70$ | |
| 26°43 | Translation down | 2.00 | 0.48 | 1.34 |
| | Supination | 2.14 | −1.53 | 2.33 |
| 26°43 | Translation up | 0.07 | 0.26 | 0.13 |
| | Pronation | −0.28 | 0.64 | 0.33 |
| | Full-cycle average | 1.00 | 0.10 | 0.93 |
| | Advanced rotation | | $\beta = 46^\circ30$ | |
| 30°88 | Translation down | 2.42 | 0.67 | 1.79 |
| | Supination | 3.32 | −3.76 | 9.03 |
| 30°88 | Translation up | 0.11 | 0.57 | 0.28 |
| | Pronation | −2.37 | 1.89 | 4.31 |
| | Full-cycle average | 1.00 | 0.10 | 2.91 |
| | Delayed rotation | | $\beta = 38^\circ93$ | |
| 30°58 | Translation down | 2.85 | 0.43 | 2.09 |
| | Supination | 0.28 | −0.73 | 0.39 |
| 30°58 | Translation up | 0.16 | 0.50 | 0.24 |
| | Pronation | −0.31 | −0.51 | −0.04 |
| | Full-cycle average | 1.00 | 0.10 | 0.84 |

**Table 5** Effect of types of rotation around mid-chord axis in forward flight with different setting angles

| $\alpha_{s0}$ | $J = 0$ | $C_v$ | $C_h$ | $C_p$ |
|---|---|---|---|---|
| | Symmetrical rotation | | $\beta = 45^\circ$ | |
| 29°76 | Translation down | 2.31 | 0.62 | 1.67 |
| | Supination | 0.75 | −0.33 | 0.49 |
| 21°12 | Translation up | −0.06 | −0.01 | 0.03 |
| | Pronation | 0.75 | −0.33 | 0.49 |
| | Full-cycle average | 1.00 | 0.10 | 0.73 |
| | Advanced rotation | | $\beta = 45^\circ$ | |
| 32°27 | Translation down | 2.74 | 0.63 | 2.08 |
| | Supination | 0.86 | −1.58 | 1.43 |
| 27°30 | Translation up | 0.07 | 0.32 | 0.16 |
| | Pronation | −0.48 | 0.26 | 0.37 |
| | Full-cycle average | 1.00 | 0.10 | 1.05 |
| | Delayed rotation | | $\beta = 45^\circ$ | |
| 32°27 | Translation down | 2.74 | 0.63 | 2.08 |
| | Supination | −0.48 | 0.26 | 0.37 |
| 27°30 | Translation up | 0.07 | 0.32 | 0.16 |
| | Pronation | 0.86 | −1.58 | 1.43 |
| | Full-cycle average | 1.00 | 0.10 | 1.05 |

**Table 6** Effect of types of rotation around mid-chord axis in forward flight with symmetrical setting angles

| $\alpha_{s0}$ | $J = 0.5$ | $C_v$ | $C_h$ | $C_p$ |
|---|---|---|---|---|
| | Symmetrical rotation | | $\beta = 37^\circ35$ | |
| 26°23 | Translation down | 2.16 | 0.40 | 1.43 |
| | Supination | 0.75 | −0.35 | 0.53 |
| 26°23 | Translation up | 0.09 | 0.25 | 0.12 |
| | Pronation | 0.75 | −0.35 | 0.53 |
| | Full-cycle average | 1.00 | 0.10 | 0.70 |
| | Advanced rotation | | $\beta = 40^\circ40$ | |
| 30°11 | Translation down | 2.67 | 0.49 | 1.94 |
| | Supination | 0.83 | −1.59 | 1.53 |
| 30°11 | Translation up | 0.14 | 0.48 | 0.23 |
| | Pronation | −0.46 | 0.27 | 0.32 |
| | Full-cycle average | 1.00 | 0.10 | 1.03 |
| | Delayed rotation | | $\beta = 40^\circ40$ | |
| 30°11 | Translation down | 2.67 | 0.49 | 1.94 |
| | Supination | −0.46 | 0.27 | 0.32 |
| 30°11 | Translation up | 0.14 | 0.48 | 0.23 |
| | Pronation | 0.83 | −1.59 | 1.53 |
| | Full-cycle average | 1.00 | 0.10 | 1.03 |

When the axis of wing rotation is at mid-chord position, the corresponding setting angles are slightly smaller respectively for all three types of wing rotation as shown in Table 5 and Table 6. However the results in Table 6 show that symmetrical rotation around mid-chord axis is the most efficient flapping mechanism in forward flight and it consumes only 84% of the power required by delayed rotation around quarter-chord axis. Comparing all cases of possible types of rotation at different axis positions and with different ways of setting

wing angles, symmetrical rotation around mid-chord axis with symmetrical setting angles requires minimum power coefficient of 0.70 at advance ratio of 0.5. In general, advanced rotation is most inefficient.

Another variable of interest in this study is the time ratio between steady translational phase interval and total time of each stroke. This time ratio $T_t$ could vary from 0 to 1.

To produce the same vertical force $C_v = 1.0$ and the same corresponding horizontal force $C_h = 0.10$ in forward flight of advance ratio $J = 0.5$, for each time ratio $T_t$ different values of inclined stroke angle $\beta$ and corresponding setting angles $\alpha_{s1}$ and $\alpha_{s2}$ are found for symmetrical and delayed rotations at the quarter-chord axis.

The resulting power coefficient $C_p$ for delayed and symmetrical rotations around the mid-chord axis are plotted against time ratio $T_t$ in Fig. 16. There is little difference between the power coefficients for symmetrical setting angles and different setting angles. The flapping wing with delayed rotation consumes minimum power around a time ratio of 0.85. The flapping wing with symmetrical rotation consumes slightly less power as time ratio increases toward 1. In fact for both types of rotation, as translational time interval increases toward 1, rotational time interval decreases toward zero hence large frictional power due to rotation must be taken into account.

## 6 Quasi-steady results for possible flight regions

It is interesting to find that in order to sustain the same weight in forward flight with a given advance ratio $J$ and to produce the required corresponding horizontal force $C_h$, there is only one solution of inclined stroke angle $\beta$ for each type of rotation with symmetrical setting angles $\alpha_{s1} = \alpha_{s2}$ and the results are shown by the lower lines in Fig. 17. It is possible to produce enough vertical force $C_v$ but larger-than-required horizontal force $C_h$ at a given advance ratio $J$ when the inclined stroke angle $\beta$ becomes larger than this lower limit. However if the inclined stroke angle $\beta$ becomes larger than an upper limit, the wing could not produce enough vertical force. The regions between the lines shown in Fig. 17 are possible flight regions of corresponding types of rotation with symmetrical setting angles $\alpha_{s1} = \alpha_{s2}$.

With different setting angles $\alpha_{s1} \neq \alpha_{s2}$ the possible flight regions are much larger as shown in Fig. 18. With flexibility of adjusting different setting angles, it is possible to produce enough vertical force $C_v$ and required horizontal force $C_h$ at a given advance ratio $J$ for a wide range of inclined stroke angle $\beta$ in the possible flight regions.

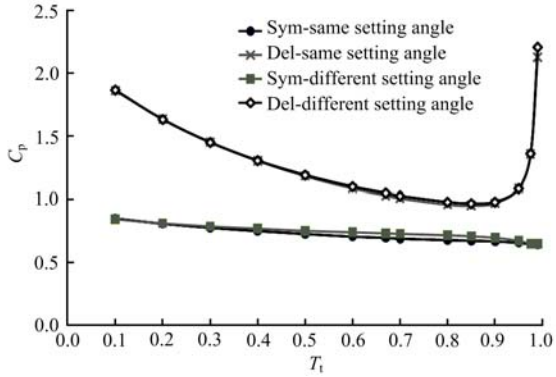


**Fig. 16** Effect of translational time interval on power consumption.

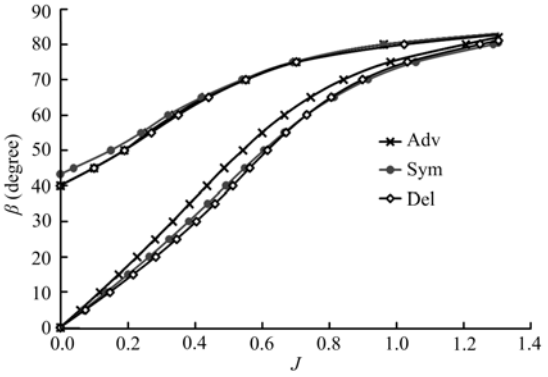


**Fig. 17** Possible flight regions for symmetrical setting angles.

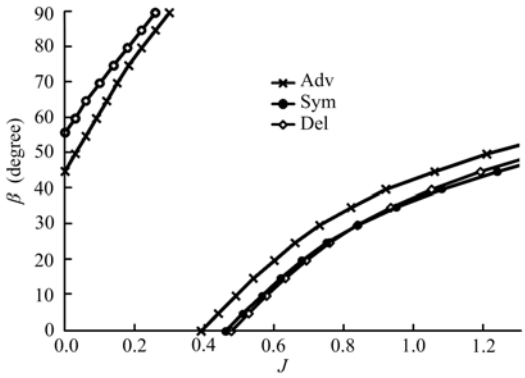


**Fig. 18** Possible flight regions for different setting angles.

## 7 Discussions

In this "modified quasi-steady" approach, 2D aerodynamic models of flapping wing motions are analyzed with focus on different types of wing rotation and different positions of rotation axis to explain the force peak at the end of each half stroke. This modification produces augmented forces around the end of each stroke.

For each case of the flapping wing motions with various combination of controlled translational and rotational velocities of the wing along inclined stroke planes with thin figure-of-eight trajectory, solutions of stroke inclined angle and setting wing angles are sought to satisfy required vertical force $C_v$ and required horizontal force $C_h$ at a given advance ratio $J$. Time-average values of non-dimensional power are calculated for efficiency analysis. From the above results, it is clear that advanced rotation is most inefficient.

In hovering flight, the results of this modified quasi-steady model are in general agreement with the unsteady results of Sun and Tang[13] and Wu and Sun[14] on the effect of positions of rotation axis and on peak forces near the end of each wing stroke. However this modified quasi-steady approach provides a systematic analysis of various parameters and their effects on efficiency of flapping wing mechanism.

Since the ratio of body drag of insect to its weight is equal to the ratio of horizontal thrust coefficient to vertical lift coefficient and this force ratio varies with advance ratio as shown in Fig 13. When body weight of insect becomes larger due to its size, it can be converted to non-dimensional vertical lift coefficient, then its effect on efficiency of flapping wing mechanisms can be better investigated in terms of force coefficient and power coefficient than in terms of body mass[15].

The results of possible flight regions shown in Fig. 17 and Fig. 18 are the most comprehensive ones. They provide insight into the possibility of hovering flight with an inclined stroke angle up to 55°. For symmetrical setting angles, forward flight can be possible only with an inclined stroke plane. However, with flexibility of adjusting different setting angles, efficient forward flight can be possible with a horizontal stroke plane for advance ratio up to 0.45.

From these "modified quasi-steady" approximate results, CFD simulation could be focused on areas and conditions of a very efficient flapping mechanism.

This "modified quasi-steady" approach could be developed for 3D model of flapping wing mechanism by a method similar to blade element theory for oscillating propeller blades.

## 8 Conclusions

The results of the "modified quasi-steady" approach of this paper provide a reasonable explanation of the force peaks around the end of each half stroke for flapping wing mechanism. This "modified quasi-steady" approach provides a systematic and comprehensive analysis of various parameters and their effects on the efficiency of flapping wing mechanism. For both hovering and forward flight, the flapping wing mechanism with symmetrical rotation around mid-chord axis is the most efficient one. A flapping mechanism with delayed rotation around the quarter-chord axis is also efficient and can be made simple by a passive rotation mechanism so that it can be useful for robotic application.

## Acknowledgement

This work is supported by the Korean Research Foundation Grant funded by the Korean Government (MOEHRD) (KRF-2006-613-D00002 and KRF-2006-005-J03301).

## References

[1] Ellington C P. The novel aerodynamics of insect flight: Application to micro-air vehicles. *Journal of Experimental Biology*, 1999, **202**, 3439–3448.

[2] Ansari S A, Zbikowski R, Knowels K. Aerodynamics modeling of insect-like flapping flight for micro air vehicles. *Progress in Aerospace Science*, 2006, **42**, 129–172.

[3] Dickinson M H, Lehmann F O, Sane S P. Wing rotation and the aerodynamics basis of insect flights. *Science*, 1999, **284**, 1954–1960.

[4] Lehmann F O. The mechanisms of lift enhancement in insect flight. *Naturwissenschaften*, 2004, **91**, 101–122.

[5] Ellington C P. The aerodynamics of hovering insect flight, II: Morphological parameters. *Philosophical Transactions of the Royal Society of London*, 1984, **305**, 17–40.

[6] Sane S P, Dickinson M H. The aerodynamic effects of wing rotation and a revised quasi-steady model of flapping flight.

*Journal of Experimental Biology*, 2002, **205**, 1087–1096.

[7] Sane S P. The aerodynamics of insect flight. *Journal of Experimental Biology*, 2003, **206**, 4191–4208.

[8] Wang Z J, Birch J M, Dickinson M H. Unsteady forces and flows in low Reynolds number hovering flight: Two-dimensional computations vs robotic wing experiments. *Journal of Experimental Biology*, 2004, **207**, 449–460.

[9] Dickinson M H, Gotz K G. Unsteady aerodynamic performance of model wings at low Reynolds numbers. *Journal of Experimental Biology*, 1993, **174**, 45–64.

[10] Isaac K M, Shivaram P, DalBello T. Low Re, high aerodynamics with controlled wing kinematics. *The* 33*rd Fluid Dynamics Conference and Exhibit*, Orlando, 2003.

[11] Nachtigall W, Hanauer-Thieser U. Flight of the honeybee, V. *Journal of Comparative Physiology B*, 1992, **162**, 267–277.

[12] Dudley R, Ellington C P. Mechanics of forward flight in bumblebees, II: Quasi-steady lift and power requirements. *Journal of Experimental Biology*, 1990, **148**, 53–88.

[13] Sun M, Tang J. Unsteady aerodynamic force generation by a model fruit fly wing in flapping motion. *Journal of Experimental Biology*, 2002, **205**, 55–70.

[14] Wu J H, Sun M. Unsteady aerodynamic forces of a flapping wing. *Journal of Experimental Biology*, 2004, **207**, 1137–1150.

[15] Lehmann F O. The constraints of body size on aerodynamics and energetics in flying fruit flies: An integrative view. *Zoology*, 2002, **105**, 287–295.